

Power Modeling in mm-Wave and Terahertz CMOS Transmitters for Wireless Network-on-Chip

Mohammad Shahmoradi¹, Korkut Kaan Tokgöz², Eduard Alarcón¹, and Sergi Abadal¹

¹Universitat Politècnica de Catalunya, Barcelona, Spain

²Sabancı University, Istanbul, Turkey

Abstract—Wireless Network-on-Chip (WNoC) systems, which interconnect chips using wireless links, face significant challenges in area and power consumption. To tackle these constraints, behavioral models (BMs) are crucial for assessing system performance under various conditions and optimizing parameters like data throughput and power consumption. Building transceivers (TRXs) physically is costly and time-consuming, making modeling a more practical approach. This paper develops a power consumption model for the sub-blocks of a WNoC transmitter (TX) at the chip level. By integrating these BMs with MATLAB, we aim to create a power model for TXs in WNoC architectures, optimized for CMOS technology operating at millimeter-wave and terahertz frequencies.

Index Terms—Wireless Network-on-Chip, Behavioral Models, Power Consumption, Millimeter-wave, Terahertz, CMOS.

I. INTRODUCTION

The demand for bandwidth in wireless communication systems has surged over recent decades, primarily due to the rise of data-intensive applications. According to Edholm’s law [1], bandwidth and data rates approximately double every 18 months. Consequently, current wireless networks are approaching capacity limits, intensifying the need for larger spectral bandwidth to support higher data rates [2].

As lower-frequency bands become congested in 6G networks and beyond, there is a growing need to explore higher-frequency bands, such as millimeter-wave (mm-Wave) and terahertz (THz) frequencies, to support future data demands [3], [4]. These higher frequencies offer increased bandwidth and data rates but also introduce signal propagation and system design challenges [3], [5]–[7].

Transitioning to THz frequencies allows for smaller antennas and transceivers (TRXs), enabling applications previously unfeasible [8], such as Wireless Network-on-Chip (WNoC). WNoC refers to the wireless interconnection of chip components like CPUs, GPUs, and memory, enhancing communication speed and flexibility [9], [10]. Figure 1 illustrates the WNoC architecture, emphasizing its transmitter (TX) blocks including an amplifier, mixer, oscillator, modulator, and filters.

However, developing WNoC systems involves stringent power and area constraints, requiring efficient design [11]. Behavioral modeling of electronic components facilitates simulation of sub-block performance under realistic conditions,

The authors acknowledge support from the European Commission through grants HORIZON-EIC-2022-PATHFINDEROPEN-01-101099697 (“QUADRATURE”), HORIZON-ERC-2021-101042080 (“WINC”), and HORIZON-MSCA-2022-PF-101062272 (“ENSPEC6G”), as well as from TÜBİTAK through grant 121C073.

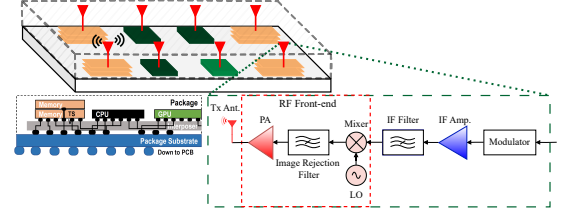


Fig. 1: Wireless Network-on-Chip (WNoC) architecture in a multi-chip system, with the detail of an integrated transmitter.

mitigating the need for costly prototyping [12], [13]. Traditional modeling techniques such as S-parameters [14], thermal noise analysis [15] or VHDL-AMS [16] provide valuable insights and allow for predictions of system performance.

Recent efforts in behavioral modeling have targeted mm-wave and THz systems, which are critical for achieving high data rates in future wireless technologies [17]–[21], but not directly applicable to WNoC systems. WNoC theoretically offers flexibility in selecting the frequency band of operation, due to the ultra-short range and potential use of metallic enclosures to avoid signal leakage outside the chip package; but existing models typically focus on specific frequency bands. Moreover, existing BMs often focus on individual components, neglecting system-level interactions necessary for understanding power consumption trends in WNoC. Thus, there is a need for a comprehensive model encompassing entire TX sub-blocks, which can predict power consumption as a function of the operating frequency before physical implementation.

In this context, this paper introduces a behavioral modeling method for predicting the power consumption of integrated transmitters in WNoC systems, specifically targeting mm-wave and THz bands as a function of operating frequency. The model captures the power dynamics of essential transmitter components such as Power Amplifiers (PAs), mixers, and oscillators – offering a comprehensive analysis of how frequency influences power consumption. By addressing the specific challenges of THz frequencies, where standards and frequency bands remain underdeveloped, this model provides a valuable tool for exploring the design space of WNoC systems, toward demonstrating the value and feasibility.

The remainder of this paper is organized as follows: Sec. II outlines the methodology for deriving power models of the PA, mixer, and oscillator. Sec. III presents the results and analyzes the model’s performance. Finally, Sec. IV summarizes the key findings and suggests future research directions.

II. METHODOLOGY

WNoC systems are constrained by both area and power, with no specific frequency allocations currently defined for their operation. To address this limitation, developing BMs that predict power consumption behavior as a function of frequency provides a valuable tool for designers working within these constraints. In this work, we focus on modeling the power consumption of three key components of a transmitter—namely the power amplifier, oscillator, and mixer—across different operating frequencies. These components are fundamental to virtually all modulation schemes. The model focuses on the relationship between operating frequency and power consumption within the mm-wave and THz frequency bands, targeting CMOS-based implementations.

MATLAB was used to extract the power models to fit the power behavior as a frequency function for both individual sub-blocks and the entire transmitter chain. To develop the power models, we leveraged comprehensive surveys on PAs and oscillators conducted by ETH Zurich [22], while data for the mixers was initially gathered from [23] and subsequently expanded [24]–[31]. Based on these surveys, we identified key parameters within each sub-block and established meaningful relationships between them. This allowed us to create appropriate Figures of Merit (FOMs) for extracting the power model of each component, as described in the next subsections.

A. Power Amplifier

Since the power amplifier is the most power-intensive component among the transceiver sub-blocks, it was prioritized in the modeling process. To develop a model for the DC power consumption (P_{DC}) of the power amplifier, establishing a reliable benchmark is crucial. A valuable resource for this is the comprehensive survey conducted by ETH Zurich [22], which provides an extensive dataset of various key features. One of them is Power-Added Efficiency (PAE), a critical parameter that inherently accounts for P_{DC} . The survey focuses on those manufactured using widely available technologies, such as bulk CMOS, SiGe, and GaAs. Additionally, it includes information on sub-THz/THz fundamental and harmonic oscillators, all of which are relevant to emerging research in beyond-5G/6G applications. These devices are particularly relevant to our goal of power modeling, as PAE is directly related to P_{DC} ,

$$PAE = \frac{P_{out}^{mW} - P_{in}^{mW}}{P_{DC}^{mW}}. \quad (1)$$

To analyze the behavior of P_{DC} as a function of operating frequency, it is essential to obtain values for the targeted output power P_{out} and input power P_{in} , as these cannot be directly substituted with gain values expressed in decibels (dB) from the survey. The data collected in the survey provides information on both PAE and P_{DC} . For our analysis, we will assume three distinct P_{in} levels at -20, 10, and 0 dBm and a P_{out} level of 0 dBm to develop a thorough BM for the power amplifiers (or their absence). In the initial step, we assume a constant value for P_{out} ; however, through the modeling process, this will be derived from the link budget

analysis in future works. Using linear regression techniques in MATLAB, we can establish a frequency-dependent power model for power amplifiers, based on the scatter plot data.

B. Oscillator

Fundamental oscillators are preferred for computational units due to their superior power efficiency, which is essential for managing thermal constraints. Unlike harmonic oscillators, which demand more complex and power-intensive circuitry, fundamental oscillators offer an efficient solution without compromising performance.

A similar approach to power amplifiers, as described in Section II-A, was initially adopted for oscillator modeling. The process was informed by the survey conducted in [22], which focused on oscillators operating above 104 GHz. However, gaps in the available data were identified and addressed. To mitigate these gaps, we have been developing a survey specifically tailored to our study, focusing on fundamental oscillators operating within the 12.7 GHz to 272 GHz frequency band [32]–[38].

Several FOMs are available [39] to model the power consumption of oscillators. The most relevant for our purpose is

$$FOM_{Osc} = PN + 10 \log_{10} \frac{P_{DC}}{1 \text{ mW}} - P_{out} - 20 \log_{10} \frac{f_o}{\Delta f}, \quad (2)$$

where PN , f_o , and Δf represent the phase noise (dBc/Hz), oscillation frequency (GHz), and frequency offset (MHz), respectively. When Equation (2) is plotted as a function of operating frequency, no clear or meaningful trend emerges from this benchmark value alone. However, by focusing on Equation (2) and deriving sub-FOMs, a more refined metric is obtained. The most effective is the DC-to-RF efficiency,

$$\text{DC-to-RF Efficiency} = \frac{P_{RF, Osc.}}{P_{DC, Osc.}}. \quad (3)$$

Based on the assumptions regarding P_{in} for the power amplifiers in Section II-A, as well as to ensure a comprehensive model, we analyzed three distinct levels for $P_{RF, Osc.}$: -20 dBm, -10 dBm, and 0 dBm. Ultimately, a specific value for $P_{RF, Osc.}$ was selected for our transmitter power modeling. This approach enabled us to derive an oscillator power model as a function of the operating frequency.

C. Mixer

To complete the modeling of the RF front-end sub-blocks of the transmitter, a thorough investigation was undertaken on mixers, with a particular emphasis on their P_{DC} consumption. Notably, a comprehensive analysis of mixers has not been extensively explored in prior works. Following a similar approach to the power amplifier analysis, we identified a significant correlation between the Conversion Gain (CG) and the P_{DC} in mixers. Therefore, for the power modeling of mixers, we used the conversion gain,

$$CG \text{ (dB)} = 10 \log_{10} \left(\frac{P_{RF, out}}{P_{IF, in}} \right). \quad (4)$$

To obtain the specific CG to use, we assume a fixed $P_{IF, in}$ and, based on the assumptions outlined in Section II-A three

levels of $P_{RF,out}$ (-20, -10, and 0 dBm). Once the CG is calculated, we can extract the power consumption of the mixer as a function of operating frequency.

III. RESULTS

In this section, we present the results of applying our survey-based modeling approach and integrate the power models of individual sub-blocks as a function of frequency (where f in all figures represents frequency). This results in a comprehensive behavioral model for the entire transmitter chain, optimized for WNoC applications.

A. Power Amplifier

Given that this work relies on data from the survey to determine the relevance of various features, statistical methods play a crucial role in identifying the most suitable FOM. One such method is calculating the correlation between different parameters, with the results presented in Table I. These calculations enable us to maximize accuracy in selecting and refining the merit coefficient, ensuring a more precise and reliable model. A review of the data in Table I allowed us to comprehend a notable correlation between the saturated power P_{sat} and PAE.

TABLE I: Correlation matrix of the power amplifier features

	P_{sat} [dBm]	PAE [%]	Gain [dB]	Area [mm ²]
P_{sat} [dBm]	1.00	0.42	0.18	0.15
PAE [%]	0.42	1.00	0.06	0.02
Gain [dB]	0.18	0.06	1.00	-0.07
Area [mm ²]	0.15	0.02	-0.07	1.00

After extracting the relevant FOM for the power amplifiers from the survey (i.e. PAE), we first plotted and fitted the PAE against the operating frequency using an exponential curve, as shown in Figure 2. The regression curve marked as *Reg*, reveals a clear trend, with scattered data points color-coded according to their specific characteristics.

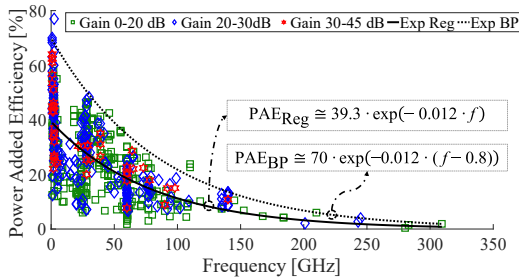


Fig. 2: PAE versus frequency based on survey's data [22]

After approximating the exponential curve with the survey's data, the maximum PAE data points were selected across all frequencies to obtain a current FOM describing the best achievable performance. This involves estimating the desired exponential curve giving a higher weight to the best points (BPs) of design. The principle behind this approach is that the higher the PAE, the less P_{DC} , Equation (1), leading to a more optimized model. Therefore, to assess the feasibility of WNoC, we target best-in-class PA designs.

For further analysis, the exponential estimation described here is based on the BPs and used to obtain P_{DC} . As shown in Figure 3, the P_{DC} increases exponentially with rising operating frequency. At high frequencies and requiring a gain of 20 dB, the power consumption of the PA can reach a few hundred mWs.

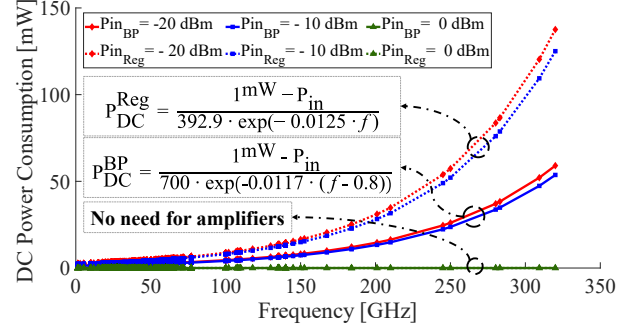


Fig. 3: PA power model as a function of frequency.

B. Oscillator

Following the procedure outlined in Section III-A, we employed regression analysis to identify a parabolic or exponential trend line for the oscillators, selecting BPs to ensure curve accuracy. Utilizing the DC-to-RF efficiency from Equation (3), we derived the behavior of P_{DC} , as illustrated in Fig. 4. Our model indicates that fundamental oscillators near 42 GHz achieve improved DC-to-RF efficiency; however, those operating in the mm-wave and THz ranges require higher DC power, resulting in efficiency losses.

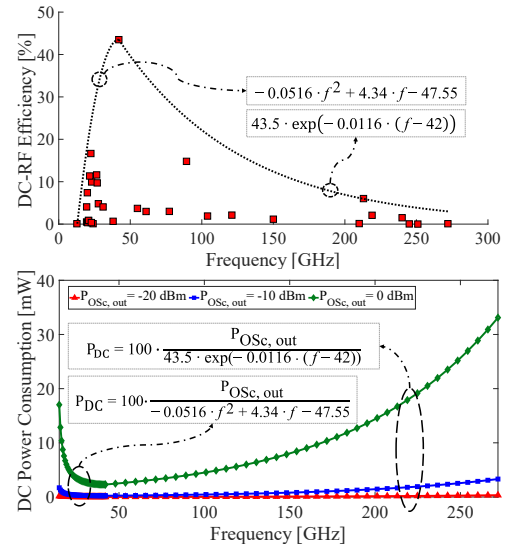


Fig. 4: Fundamental oscillator DC-RF efficiency as a function of the frequency (top) and resulting power consumption in multiple output power configurations (bottom).

At lower frequencies, resistive parasitic losses and the energy needed to sustain oscillation limit RF output, further reducing efficiency [40], [41]. The fitting line reflects an initial parabolic increase in efficiency, peaking at 42 GHz, followed by an exponential decline, with P_{DC} staying below 35 mW.

C. Mixer

The relationship between conversion gain and power consumption was plotted and fitted across the entire spectrum, revealing a trend similar to that of oscillators in Section III-B. Figure 5 presents the power model for mixers as a function of operating frequency, and the resulting power consumption.

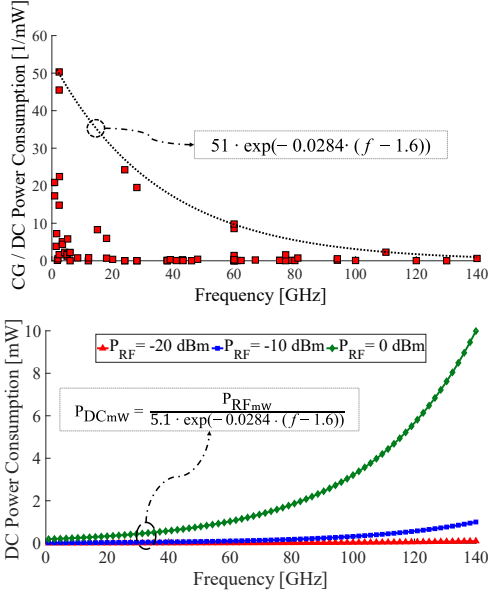


Fig. 5: Mixer power consumption model as a function of frequency (top) and resulting P_{DC} (bottom).

The model follows a clear negative exponential trend with frequency, which leads to an exponentially increasing power consumption, which is especially notable when the mixer needs to provide higher output power (remember that we fix $P_{IF, in}$ to a constant value).

D. Transmitter Chain

By modeling the individual TX sub-blocks, developing a comprehensive BM for the TX chain becomes feasible. Each sub-block has been thoroughly analyzed, detailing power as a function of operating frequency across four levels of mixer P_{out} and a consistent oscillator $P_{RF, out}$ of -10 dBm across all frequencies. These models were integrated in MATLAB, covering the full frequency ranges of the sub-blocks. This unified BM serves as a valuable tool for predicting overall TX behavior, providing insights that can guide designers in optimizing WNoC systems.

Given the operating frequency limitations observed in surveys of power amplifiers (up to 320 GHz), mixers (up to 140 GHz), and oscillators (up to 272 GHz) in CMOS technology, we selected four specific frequencies (see Figure 6). We chose 28 GHz and 60 GHz due to their established maturity among power amplifiers, known as the most power-intensive components. However, due to limitations in mixer data, we selected 140 GHz, and since 243 GHz has been the focus of several important studies, it was also included. It should be mentioned that the contribution of the mixer at 243 GHz is extrapolated.

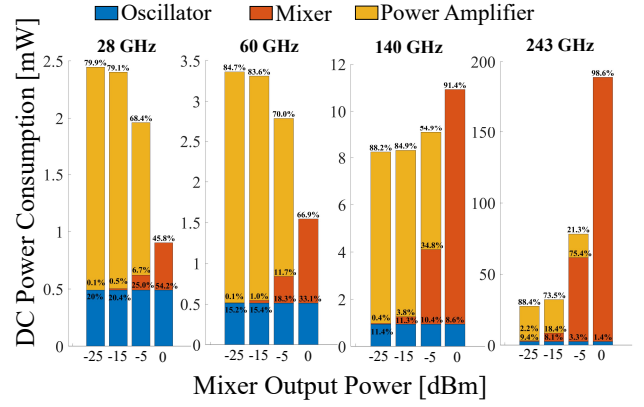


Fig. 6: DC power contribution of the TX front-end across frequencies, assuming different mixer P_{out} levels, with PA and oscillator P_{out} set to 0 dBm and -10 dBm, respectively.

As shown in Figure 6, the PA dominates the total P_{DC} , especially when the mixer's P_{out} is low (below -15 dBm), contributing over 73.5% to the total. At higher mixer P_{out} levels, such as -5 dBm, the mixer's contribution increases, reaching 34.8% and 75.4% at 140 GHz and 243 GHz, respectively. When the mixer's P_{out} is 0 dBm and no additional amplification is needed, the combined DC power consumption of the mixer at 28 GHz and 60 GHz rises to nearly 0.5 mW and 1 mW, respectively, with a corresponding decrease in the oscillator's contribution.

At elevated frequencies, such as 243 GHz, the mixer's P_{DC} contribution grows significantly while the oscillator's impact decreases. For instance, when the PA is active with a mixer P_{out} of -5 dBm, the power contributions of the PA, mixer, and oscillator are 21.3%, 75.4%, and 3.3%, respectively. In the absence of the PA (at 0 dBm mixer P_{out}), the combined P_{DC} from the mixer and oscillator at 243 GHz reaches approximately 190 mW, with contributions of 98.6% from the mixer and 1.4% from the oscillator, underscoring the mixer's significant role at higher frequencies.

Overall, the derived P_{DC} model reveals an exponential increase in power consumption with operating frequency. As both the mixer's P_{out} and the frequency rise, the contributions from the mixer grow substantially, emphasizing its impact at mm-wave and THz frequencies.

IV. CONCLUSION

This paper addresses the critical challenge of DC power consumption in WNoC systems by introducing a behavioral model tailored for CMOS-based transmitters at mm-wave and THz frequencies. By evaluating the power contributions of each transmitter sub-block, this model offers a scalable approach for predicting DC power consumption across various operating frequencies, giving designers an effective tool for optimizing power efficiency without the expense of physical prototypes. This approach supports the development of high-performance, energy-efficient WNoC architectures and advances future innovations in mm-wave and THz wireless communication transceivers.

REFERENCES

- [1] S. Cherry, "Edholm's law of bandwidth," *IEEE spectrum*, vol. 41, no. 7, pp. 58–60, 2004.
- [2] T. S. Rappaport, Y. Xing, O. Kanhere, S. Ju, A. Madanayake, S. Mandal, A. Alkhatieb, and G. C. Trichopoulos, "Wireless communications and applications above 100 ghz: Opportunities and challenges for 6g and beyond," *IEEE access*, vol. 7, pp. 78 729–78 757, 2019.
- [3] S. Ali, M. Sohail, S. B. H. Shah, D. Koundal, M. A. Hassan, A. Abdollahi, and I. U. Khan, "New trends and advancement in next generation mobile wireless communication (6g): a survey," *Wireless Communications and Mobile Computing*, vol. 2021, no. 1, p. 9614520, 2021.
- [4] P. Chatzimisios, D. Soldani, A. Jamalipour, A. Manzalini, and S. K. Das, "Special issue on 6g wireless systems," *Journal of Communications and Networks*, vol. 22, no. 6, pp. 440–443, 2020.
- [5] J. Crols and M. Steyaert, *CMOS wireless transceiver design*. Springer Science & Business Media, 2013, vol. 411.
- [6] J. Du Preez, S. Sinha, and K. Sengupta, "Sige and cmos technology for state-of-the-art millimeter-wave transceivers," *IEEE Access*, 2023.
- [7] D. L. Woolard, R. Brown, M. Pepper, and M. Kemp, "Terahertz frequency sensing and imaging: A time of reckoning future applications?" *Proceedings of the IEEE*, vol. 93, no. 10, pp. 1722–1743, 2005.
- [8] S. Abadal, C. Han, V. Petrov, L. Galluccio, I. F. Akyildiz, and J. M. Jornet, "Electromagnetic nanonetworks beyond 6g: From wearable and implantable networks to on-chip and quantum communication," *IEEE Journal on Selected Areas in Communications*, 2024.
- [9] S. Abadal, R. Guirado, H. Taghvaei, A. Jain, E. P. de Santana, P. H. Bolívar, M. Saeed, R. Negra, Z. Wang, K.-T. Wang *et al.*, "Graphene-based wireless agile interconnects for massive heterogeneous multi-chip processors," *IEEE Wireless Communications*, 2022.
- [10] S. H. Gade and S. Deb, "Hywin: Hybrid wireless noc with sandboxed sub-networks for cpu/gpu architectures," *IEEE Transactions on computers*, vol. 66, no. 7, pp. 1145–1158, 2016.
- [11] S. Abadal, M. Iannazzo, M. Nemirovsky, A. Cabellos-Aparicio, H. Lee, and E. Alarcón, "On the area and energy scalability of wireless network-on-chip: A model-based benchmarked design space exploration," *IEEE/ACM Transactions on Networking*, vol. 23, no. 5, pp. 1501–1513, 2014.
- [12] F. M. Ghannouchi, O. Hammi, and M. Helaoui, *Behavioral modeling and predistortion of wideband wireless transmitters*. John Wiley & Sons, 2015.
- [13] K. Lahiri, A. Raghunathan, and S. Dey, "System-level performance analysis for designing on-chip communication architectures," *IEEE Transactions on Computer-Aided Design of Integrated Circuits and Systems*, vol. 20, no. 6, pp. 768–783, 2001.
- [14] Z. He and S. Zhou, "Bpnn-based behavioral modeling of the s-parameter variation characteristics of pas with frequency at different temperatures," *Micromachines*, vol. 13, no. 11, p. 1831, 2022.
- [15] T. J. Eguia, S. X.-D. Tan, R. Shen, E. H. Pacheco, and M. Tirumala, "General behavioral thermal modeling and characterization for multi-core microprocessor design," in *2010 Design, Automation & Test in Europe Conference & Exhibition (DATE 2010)*. IEEE, 2010, pp. 1136–1141.
- [16] J. Hinojosa, G. Doménech-Asensi, and J. Martínez-Alajarín, "Development of vhdl-ams neuro-fuzzy behavioral models for rf/microwave passive components," *Int. J. RF Microwave Comput.-Aided Eng.*, vol. 17, no. 3, pp. 335–344, 2007.
- [17] S. U. Ghazati, A. Baddeley, and R. Quaglia, "Large-signal characterization and behavioral modeling of mm-wave gan hemt switches tailored for advanced power amplifier architectures," in *IEEE Topical Conf. on RF/Microwave Power Amplifiers for Radio and Wireless Applications (PAWR)*. IEEE, 2024, pp. 21–23.
- [18] S. Wu, X. Li, T. Tan, and Z. Huang, "Optimized design of low-noise amplifier based on behavior-level parameter modeling," in *2023 International Conference on Microwave and Millimeter Wave Technology (ICMMT)*. IEEE, 2023, pp. 1–3.
- [19] P. Taghikhani, *Modeling Approaches for Active Antenna Transmitters*. Chalmers Tekniska Hogskola (Sweden), 2021.
- [20] J. M. Jornet, V. Petrov, H. Wang, Z. Popović, D. Shakya, J. V. Siles, and T. S. Rappaport, "The evolution of applications, hardware design, and channel modeling for terahertz (thz) band communications and sensing: Ready for 6g?" *Proceedings of the IEEE*, 2024.
- [21] N. Chukhno, O. Chukhno, D. Moltchanov, S. Pizzi, A. Gaydamaka, A. Samuylov, A. Molinaro, Y. Koucheryavy, A. Iera, and G. Araniti, "Models, methods, and solutions for multicasting in 5g/6g mmwave and sub-thz systems," *IEEE Communications Surveys & Tutorials*, 2023.
- [22] H. Wang, M. Eleraky, B. Abdelaziz, B. Lin, E. Liu, Y. Liu, M. Ghorbanpoor, C. Chu, A. Ruffino, J. Xu, F. Svelto, N. Villaggi, A. Habib, K. Choi, T.-Y. Huang, H. Jalili, N. S. Mannem, J. Park, J. Lee, D. Munzer, S. Li, F. Wang, A. S. Ahmed, C. Snyder, H. T. Nguyen, and M. E. D. Smith. (2020) Power amplifiers performance survey 2000-present. [Online; accessed 10-October-2024]. [Online]. Available: <https://ideas.ethz.ch/research/surveys/pa-survey.html>
- [23] H. Zhang, S. Tang, M. Cai, and Y. Jiang, "Optimal design of cmos mixer: A research review," *International Journal of RF and Microwave Computer-Aided Engineering*, vol. 32, no. 12, p. e23531, 2022.
- [24] Y. Peng, J. He, H. Hou, H. Wang, S. Chang, Q. Huang, and Y. Zhu, "A K -band high-gain and low-noise folded cmos mixer using current-reuse and cross-coupled techniques," *IEEE Access*, vol. 7, pp. 133 218–133 226, 2019.
- [25] H. Duan, J. Chen, M. Wang, H. Wei, Q. Zhang, and H. Quan, "High linearity wide band passive mixer for ku-band applications in a 180nm cmos technology," in *2022 7th International Conference on Integrated Circuits and Microsystems (ICICM)*. IEEE, 2022, pp. 565–569.
- [26] B. R. Jackson and C. E. Saavedra, "A cmos ku-band 4x subharmonic mixer," *IEEE Journal of Solid-State Circuits*, vol. 43, no. 6, pp. 1351–1359, 2008.
- [27] D. Cheng, L. Li, M. Xie, B. Sheng, and X. You, "A ku-band receiver with 12-to-20-db gain, -14-dbm ipldb in 65-nm cmos technology," in *2018 Asia-Pacific Microwave Conference (APMC)*, 2018, pp. 765–767.
- [28] Y. Wang, L. Lou, B. Chen, Y. Zhang, K. Tang, L. Qiu, S. Liu, and Y. Zheng, "260-mw ku-band fmcw transceiver for sar sensor with 1.48-ghz bw in 65-nm cmos," *IEEE Trans. Microw. Theory Tech.*, vol. 65, no. 11, pp. 4385–4399, 2017.
- [29] F. Zhang, E. Skafidas, W. Shieh, B. Yang, B. N. Wicks, and Z. Liu, "A 60-ghz double-balanced mixer for direct up-conversion transmitter on 130-nm cmos," in *2008 IEEE Compound Semiconductor Integrated Circuits Symposium*, 2008, pp. 1–4.
- [30] Y.-S. Lin, R.-C. Liu, C.-C. Wang, and C.-C. Chen, "A low power and high conversion gain 77–81 ghz double-balanced up-conversion mixer with excellent lo-rf isolation in 90 nm cmos," in *2015 IEEE Radio and Wireless Symposium (RWS)*, 2015, pp. 171–173.
- [31] Y.-S. Lin, K.-S. Lan, C.-C. Wang, C.-C. Chi, and S.-S. Lu, "6.3 mw 94 ghz cmos down-conversion mixer with 11.6 db gain and 54 db lo-rf isolation," *IEEE Microwave and Wireless Components Letters*, vol. 26, no. 8, pp. 604–606, 2016.
- [32] Y. Li, X. Wu, J. Gu, Q. J. Gu, Z. Xu, and X. Yu, "A k-band cmos standing wave oscillator using digital-controlled artificial dielectric differential transmission lines," *IEEE Microwave and Wireless Components Letters*, vol. 32, no. 10, pp. 1195–1198, 2022.
- [33] I. Mansour, M. Mansour, M. Aboualalaa, and R. K. Pokharel, "Design of low phase noise k-band vco using high quality factor resonator in 0.18 μm cmos technology," *International Journal of RF and Microwave Computer-Aided Engineering*, vol. 32, no. 4, p. e23045, 2022.
- [34] I. Mansour, M. Mansour, A. Allam, and A. B. Abdel-Rahman, "A 2.2-mw 23 ghz cmos vco using high-quality factor complementary split ring resonator with a- 195dbc/hz fom," *AEU-International Journal of Electronics and Communications*, vol. 155, p. 154356, 2022.
- [35] Y. Huang, Y. Chen, H. Guo, P.-I. Mak, and R. P. Martins, "A 3.3-mw 25.2-to-29.4-ghz current-reuse vco using a single-turn multi-tap inductor and differential-only switched-capacitor arrays with a 187.6-dbc/hz fom," *IEEE Trans. Circuits Syst. I: Reg. Papers*, vol. 67, no. 11, pp. 3704–3717, 2020.
- [36] Y. Fu, L. Li, D. Wang, and X. Wang, "A- 193.6 dbc/hz fom t 28.6-to-36.2 ghz dual-core cmos vco for 5g applications," *IEEE Access*, vol. 8, pp. 62 191–62 196, 2020.
- [37] L. Gomes, E. Sharma, A. A. L. Souza, A. L. C. Serrano, G. P. Rheder, E. Pistono, P. Ferrari, and S. Bourdel, "77.3-ghz standing-wave oscillator using an asymmetrical tunable slow-wave resonator," *IEEE Trans. Circuits Syst. I: Reg. Papers*, vol. 68, no. 8, pp. 3158–3169, 2021.
- [38] B. Philippe and P. Reynaert, "A 126 ghz, 22.5% tuning, 191 dbc/hz fomt 3rd harmonic extracted class-f oscillator for d-band applications in 16nm finfet," in *2020 IEEE Radio Frequency Integrated Circuits Symposium (RFIC)*. IEEE, 2020, pp. 263–266.
- [39] S. Poolakkal and N. Nallam, "Enhancing the phase-noise-figure-of-merit of a resonator using frequency transformations," in *2020 33rd International Conference on VLSI Design and 2020 19th International Conference on Embedded Systems (VLSID)*. IEEE, 2020, pp. 67–71.
- [40] T. H. Lee, *The design of CMOS radio-frequency integrated circuits*. Cambridge university press, 2003.
- [41] B. Razavi, *Fundamentals of microelectronics*. John Wiley & Sons, 2021.